Journal Pre-proofs

Thermodynamic approach to foresee experimental CO_2 reduction to organic compounds

Laura Rovira-Alsina, Meritxell Romans-Casas, M. Dolors Balaguer, Sebastià Puig

PII: S0960-8524(22)00510-7
DOI: https://doi.org/10.1016/j.biortech.2022.127181
Reference: BITE 127181

To appear in: *Bioresource Technology*

Received Date: 23 March 2022
Revised Date: 12 April 2022
Accepted Date: 14 April 2022

Please cite this article as: Rovira-Alsina, L., Romans-Casas, M., Dolors Balaguer, M., Puig, S., Thermodynamic approach to foresee experimental CO_2 reduction to organic compounds, *Bioresource Technology* (2022), doi: https://doi.org/10.1016/j.biortech.2022.127181

Thermodynamic approach to foresee experimental CO_2 reduction to organic compounds

Laura Rovira-Alsina*, Meritxell Romans-Casas*, M. Dolors Balaguer, Sebastià Puig+

LEQUiA. Institute of the Environment. University of Girona. Campus Montilivi. C/Maria Aurèlia Capmany, 69, E-17003 Girona, Catalonia, Spain.

* These authors contributed equally.

+ Corresponding author: sebastia.puig@udg.edu

Abstract

Anaerobic gas fermentation is a promising approach to transform carbon dioxide (CO_2) into chemical building blocks. However, the main operational conditions to enhance the process and its selectivity are still unknown. The main objective of this study was to trigger chain elongation from a joint perspective of thermodynamic and experimental assessment. Thermodynamics revealed that acetic acid formation was the most spontaneous reaction, followed by n-caproic and n-butyric acids, while the doorway for alcohols production was bounded by the selected conditions. Best parameters combinations were applied in three 0.12L fermenters. Experimentally, n-caproic acid formation was boosted at pH 7, 37°C, Acetate:Ethanol mass ratio of 1:3 and low H_2 partial pressure. Though these conditions did not match with those required to produce their main substrates, the unification of both perspectives yielded the highest n-caproic acid concentration (> 11 g L^{-1}) so far from simple substrates, accounting for 77% of the total products.

Keywords:

Anaerobic fermentation; carboxylate platform; chain elongation; CO_2 valorization; open culture.

1. Introduction

CO_2 can be reused as a substrate for energy, fuels and chemicals formation through different approaches. Gas fermentation (GF) is a well-known technology able to perform the recycling of CO_2 (Agler et al., 2011) into chemical building blocks using microorganisms as catalysts (Dürre and Eikmanns, 2015). Acetic acid (HA), a short-chain carboxylic acid (SCCA), is one of the most produced compounds which can be further valorised through its reduction into elongated compounds, the so-called medium-chain carboxylic acids (MCCAs, compounds from six to twelve carbons). Chain elongation is included in the carboxylate platform, set out as a second fermentation process (Agler et al., 2011) and its feasibility has been already proven (Angenent et al., 2016; Candry and Ganigué, 2021). It involves the cyclic addition of two carbon molecules to the compound-chain through the reverse β-oxidation pathway, in which an electron donor (i.e. ethanol) and an electron acceptor (i.e. an organic compound itself) are interconnected through electron transfer mechanisms (Cavalcante et al., 2017). Although pure cultures were initially employed and largely investigated, it was later demonstrated that open cultures are advantageous due to their robust and resilient communities, and their increased production rates owing to their synergistic behaviour (Pinto et al., 2021; Paquete et al., 2022). This brings the technology closer to environmental conditions and its utilization has been proven to be both, cost and energy more efficient (Pinto et al., 2021).

Elongated organic compounds have broad applications such as pharmaceutical and chemical industries (Angenent et al., 2016). MCCA produced through fermentative reduction are attractive assets since they are considered suitable energy carriers avoiding the use of fossil sources at low yields (Cavalcante et al., 2017). For instance, n-butyric acid (C_4) can be employed to produce fuels (i.e. butyl or ethyl butyrate), to manufacture plastics and as a flavouring agent (Dessì et al., 2021). In respect of n-caproic acid (C_6), it has been thoroughly investigated due to its multiple applications as an antimicrobial agent, additive for animal feed and as a potential

precursor for biofuels production (Dessì et al., 2021). In addition, its current market price is circa 3.7 $/kg, followed by other organics such as alcohols, but far much higher than other acids as acetic or propionic (Wood et al., 2021).

The formations of n-butyric (HB) and n-caproic (HC) acids have been largely studied from a broad range of substrates. Elongations from HA into HB and HC using ethanol (EtOH) as electron donor have been reported before (Romans-Casas et al., 2021). Grootscholten and colleagues (2013) compared HC production rates with and without EtOH addition from HA. Recently, the feasibility of chain elongation reactions was assessed for different fermentation pathways and reactants proportion, highlighting that higher concentrations of HB benefitted HC production (Wang et al., 2020). However, there are still many gaps in knowledge, specially related to unravelling the optimum working conditions to trigger a selective formation of one specific compound starting from CO_2. Therefore, the main challenges that hinder a competitive and efficient production remain to be overcome.

Thermodynamics deals with the relationship between different forms of energy and its conversion. It is variable, depends on many factors and involves a large number of molecules interacting intricately (Hanselmann, 1991). However, when the system reaches equilibrium, it can be described in a simpler approach that can give valuable information related to energy processes. The present study developed a thermodynamic based-model to elucidate the appropriate conditions to favour chain elongation reactions. The model was focused on the combination of four parameters: pH, temperature (T), substrates ratio and compounds titers. A set of parameters identified as optimal was subsequently tested experimentally to beat the limited knowledge of the co-effect of working conditions and biology, given that thermodynamics is conditioned by the kinetics and enzymatic capabilities of each microorganism. Fermentative tests from CO_2 were carried out adding hydrogen (H_2), HA and

EtOH that can be obtained from a bioelectrochemical system (BES) (Vassilev et al., 2022), as substrates.

2. Materials and methods

2.1 Thermodynamic analysis

A thermodynamic based-model was built considering the main gas fermentation and chain elongation reactions. They were equated stoichiometrically and the standard Gibbs free energy (ΔG^o) of the main reactions was calculated and compared with the literature (**Table 1**). The standard Gibbs free energies of formation ($\Delta_f G^o$) and the standard enthalpies of formation ($\Delta_f H^o$) were extracted from Amend and Shock (2001), Alberty (2001) and the CRC Handbook of Chemistry and Physics (Lide and Baysinger, 2004). The carboxylate chain length was limited to six carbon atoms, as with longer chain compounds the addition of electrons bonded with each additional step in the β-reverse oxidation is smaller (Lambrecht et al., 2019).

The $\Delta G^o_{T_S}$ of each reaction was corrected considering the temperature, ionic strength, pH and species' concentrations. The corrected Gibbs free energy of reactions at different temperatures ($\Delta G_{(T)}$ 25, 37 and 50 °C) was calculated using the Helmholtz equation (**Eq. 1**) where standard temperature (T_s) was 298.15 K and $\Delta H^o_{T_s}$ was calculated using the standard enthalpy of formation values of each compound taken from Kleerebezem and Van Loosdrecht (2010).

$$\Delta G_{(T)} = \Delta G^o_{T_S} \frac{T}{T_s} + \Delta H^o_{T_s} \frac{T_s - T}{T_s} \qquad \text{(Eq. 1)}$$

The effect of the ionic strength was calculated based on the extended Debye-Hückel equation (**Eq. 2**) where $\Delta G_{T(I)}$ is the corrected Gibbs free energy, x_i is the stoichiometry coefficient of each specie, $RT\alpha = 9.20483 \cdot 10^{-3}\ T - 1.28467 \cdot 10^{-5}\ T^2 + 4.95199 \cdot 10^{-8}\ T^3$, $N_{H,i}$ is the number of hydrogen atoms in the substance i, Z_i is the charge number of each specie, B = 1.5 kg ^{½} mol $^{-½}$ (empirical constant from Goldberg and Tewari, 1991) and I is the ionic strength of the solution.

$$\Delta G_{T(I)} = \Delta G_T + (\sum_r x_i * \frac{RT\alpha\left(Z_i^2 - N_{H,i}\right)I^{\frac{1}{2}}}{1 + BI^{\frac{1}{2}}}) \quad \text{(Eq. 2)}$$

The range of concentrations studied was selected considering the average concentration of ions in previous experiments. The **Eq. 3** was used to calculate the three different molal ionic strengths (0.07, 0.09 and 0.11 b) used for further calculations, in which c_i is the molal concentration of the ion *i* (mol kg^{-1}) and z_i is the charge number of that ion.

$$I = \frac{1}{2}\sum_{i=1} c_i \ z_i^2 \quad \text{(Eq. 3)}$$

The pH and the activities of products and substrates in the medium were corrected adapting the Nernst equation (**Eq. 4**), in which *R* is the gas constant (8.31 J K^{-1} mol^{-1}), *T* is the chosen temperature (25, 37 or 50 °C in K), [i] denotes the activities of reactants and products of a general reaction *aA + bB* ↔ *cC + dD* and *xH* is the stoichiometric coefficient of H^+ (Gildemyn et al., 2017), which is positive when it is on the reactants side, and negative when it is on the products side. The corrected Gibbs free energy ($\Delta G_{T,I(pH,\Pi)}$) is shortened as *ΔG'*.

$$\Delta G' = \Delta G_{T,I} + RTln\prod - RTln\left([\frac{10^{-pH}}{10^{-7}}]^{xH}\right) \qquad \prod = \frac{[C]^c\ [D]^d}{[A]^a\ [B]^b} \quad \text{(Eq. 4)}$$

Assuming that the system is dilute, the calculations were simplified by estimating the activities as molar concentrations (M), which ranged from 0.001 to 0.210 M. Regarding gaseous components, the concentration in the liquid phase was estimated considering the H_2 partial pressure (which ranged from 0.25 to 1.75 atm) and Henry's law (**Eq. 5**), where C_i is the solubility of a gas component (*i*) in a particular solvent (mol L^{-1}), H_i is Henry's law constant in mol L^{-1} atm^{-1} and P_i is the partial pressure of the gas component (*i*) in atm.

$$C_i = H_i \cdot P_i \quad \text{(Eq. 5)}$$

Then, the division of the corrected Gibbs free energy by the electron transfer events (Ne) in each reaction (ΔG Ne^{-1}) was calculated to indirectly evidence the competitiveness of the different reaction pathways according to Wu et al., (2018). By mixing variables and conditions of the model, severa l situations were depicted, but not all the data were presented to ease the understanding of the results.

2.2 Inoculum, experimental setup, and operational conditions

An enriched mixed culture that previously showed the ability to trigger chain elongation (Blasco-Gómez et al., 2021) was used to validate the outputs from the thermodynamic model. Three main fermentative tests (F1 to F3) operated under the best set of conditions to prompt HC formation were tested. They consisted of 0.12 L serum bottles, with 0.05 L of the liquid phase and 0.07 L of headspace. Each fermenter was filled with a modified ATCC1754 PETC medium (see supplementary material) and inoculated with a 20 % (*v/v*) of the culture. Three consecutive washes with the same fresh media were conducted to remove all organic carbon sources coming from the raw culture. The pH of the medium was initially fixed to 6.0 and later adjusted depending on the experimental conditions. All bottles were hermetically closed with rubber stoppers and aluminium caps.

Operational conditions were established at the beginning of each experimental test and corresponded (for F1) to the ones unravelled as optimal by the thermodynamic model for HC formation. However, F2 and F3 were performed under compromise conditions to consider biological factors. Control tests (PF 1 – PF 6) were performed to check the model results for both HA and EtOH production and its accuracy in a real scenario. The temperature was maintained constant at either 25 °C (room temperature control), 37 °C (Advanced Programmable Heated Circulator thermostat bath, AP28H200A1, Spain) or 50 °C (SI600 orbital incubator, Stuart, UK). pH was set at 5.0, 6.0 or 7.0, and adjusted throughout the operational period by adding 1M sodium hydroxide or 1M hydrochloric acid when required. The used acetic

acid to ethanol mass ratio (HA:EtOH) was 1:3 in tests where those substrates were employed, corresponding to 1 g L^{-1} and 3 g L^{-1} of HA and EtOH, respectively. The ratio was selected to favour the selectivity of HC formation (Wu et al., 2022). All fermenters were kept in agitation to promote mass transfer and under the darkness to avoid photosynthetic growth. They were sparged with a gas mixture of CO_2:H_2 (20:80 % *v/v*, Praxair, Spain) twice a week, leading to an overpressure of 1 bar to keep an anaerobic environment rich in carbon and reducing power. However, F3 was once a week fed with pure CO_2 (99.9 %, Praxair, Spain), alternating the feeding regime with the CO_2:H_2 mixture to study the effect of different H_2 partial pressures. All tests were conducted in duplicate.

2.3 Analyses and calculations

Gas- and liquid-phase samples were taken once or twice a week to track the evolution of the main reactions. To maintain a steady volume, withdrawn liquid volume was replaced by fresh medium and pH was restored when needed. Electrical conductivity and pH were measured with an electrical conductivity meter (EC-meter basic 30+, Crison, Spain) and a multimeter (MultiMeter 44, Crison, Spain), respectively. The concentration of volatile fatty acids and alcohols in the liquid phase was determined using an Agilent 7890A gas chromatograph equipped with a DB-FFAP column and a flame ionization detector. The optical density (OD) was periodically measured in absorbance units (AU) to control the growth of the microbial community with a spectrophotometer (CE 1021, 1000 Series, CECIL Instruments Ltd., UK) at a wavelength of 600 nm. The dry cell weight (DCW) was calculated by performing a regression line with the total suspended solids (TSS) of different volumes of the inoculum (1 OD = 565.75 mg L^{-1}). Gas samples were analysed by gas chromatography (490 Micro GC system, Agilent Technologies, US). The Micro GC was equipped with two columns: a CP-molesive 5A for methane (CH_4), carbon monoxide (CO), H_2, oxygen (O_2) and nitrogen (N_2) analysis, and a CP-Poraplot U for CO_2 analysis, connected to a thermal conductivity detector (TCD).

Gas pressure profiles were quantified by measuring the pressure in the headspace of the fermenters using a digital pressure sensor (differential pressure gauge, Testo 512, Spain). The concentrations of dissolved H_2 and CO_2 in the liquid media were calculated using Henry's law (**Eq. 5**).

3. Results and discussion

Given the current interest generated by bio-CO_2 recycling technologies and the production of MCCAs, the present work aimed to produce elongated compounds, as HC, under the most suitable conditions. To obtain a C_6 elongated product from H_2 and CO_2 as the only substrates, a succession of several reactions was required. First, a thermodynamic model was developed to study each reaction individually and to investigate whether these conditions allowed the production of several intermediates up to HC in concomitance. Then, these conditions were tested experimentally to shed light on how the enzymatic capabilities of the biocatalyst and the kinetics of the reaction affected this approach.

3.1 Prospects for chain elongation from CO_2 step by step

HC production from CO_2 is performed through a series of cascade reactions. The spontaneity of those reactions is given by the Gibbs free energy, though its standard value is influenced by environmental conditions. First, the ΔG°_{25} values for each intermediate reaction were corrected by temperature and ionic strength ($\Delta G_{T,I}$) and represented under different scenarios (see supplementary material). None of these variables substantially modified the spontaneity of the reactions, although the temperature had a linear effect (R^2>0.999) increasing the ΔG values between 0.23 and 0.59 kJ mol^{-1} per 1 °C depending on each reaction. HA was by difference the most thermodynamically favoured compound followed by HC and HB, EtOH, n-hexanol (HexOH) and n-butanol (ButOH). Otherwise, the ratio of the corrected $\Delta G_{T,I}$ to the number of electrons transferred in each reaction ($\Delta G_{T,I}$ Ne^{-1}) was calculated to indirectly point out the

competitiveness between pathways (Wu et al., 2018). $\Delta G_{T,I}$ Ne^{-1} ratios of most of the chain elongation reactions were close to each other except for HA formation (see supplementary material), indicating that the competition between them was noticeable, as their relative differences diminished. Moreover, the order of the $\Delta G_{T,I}$ Ne^{-1} profiles changed with respect from $\Delta G_{T,I}$ ones, with HB being more spontaneous than HC and increasing the distance between EtOH and HexOH profiles. Given that any redox reaction tends to equilibrium, it was expected that the spontaneity would also be modified by the species concentration. Hence, the effect of changing pH and concentrations of reactants and products was also considered to correct the Gibbs free energy of each reaction ($\Delta G_{T,I(pH,\Pi)}$), from now on simplified as $\Delta G'$.

The production of HA from CO_2 and H_2 was inspected as the first step of the chain reaction. **Figure 1** represents the $\Delta G'$ variation under different conditions of temperature, pH, substrate ratio of employed gases and product concentration when following the hydrogenotrophic HA formation (**Table 1, R1**). The major spontaneity turned out to occur at 25 °C, pH 7 and high hydrogen partial pressure (P_{H_2}). Higher ratios of P_{H_2}:P_{CO_2} (3:1 and 1:1) enhanced the reaction compared to lower ratios (1:3), pointing out the great importance of H_2, assumed to be the electron donor of the reaction. Conversely, a rise in HA concentration considerably decreased the negative $\Delta G'$ values, while the effect of pH was even more remarkable (lower $\Delta G'$ values when less H^+ accumulated on the product side). HA formation was favourable for all the conditions tested, though threshold conditions where a shift in the spontaneity occurred (positive $\Delta G'$ values) were calculated by the model: 50 °C, pH 5, low P_{H_2} and CO_2 availability (<0.023 M). Considering HA is one of the main substrates for the production of longer-chain carboxylates (Angenent et al., 2016), the conditions favoring its formation should be heeded throughout the process.

Two different reactions were studied concerning EtOH formation, either by employing H_2 and CO_2 as substrates or through HA conversion (**Figure 2**). $\Delta G'$ values for hydrogenotrophic EtOH

production (**Figure 2A**) were lower compared to EtOH formation through HA reduction (**Figure 2B**). This matches with the literature (Baleeiro et al., 2019; Spirito et al., 2014), but after considering the concentration of reactants and products, none of them were spontaneous for any of the parameters tested ($\Delta G' > 0$), differing from the standard ones (**Table 1, R2 and R3**).

According to the previously reported by other authors, EtOH is usually the bottleneck of chain elongation, since it is the main compound required as an electron donor. Even though $\Delta G'$ values were positive, the most favourable conditions for EtOH were similar to HA formation (25 °C and high P_{H_2}), though pH 5 decreased $\Delta G'$ values compared to pH 7. Concerning reaction R2, an EtOH concentration under 10^{-3} M was necessary to shift the $\Delta G'$ to negative values while for reaction R3 it was not possible until EtOH reached concentrations below 10^{-8} M. Nevertheless, at 50 °C $\Delta G'$ values could never surpass the spontaneity line.

Since HC is thought to be produced through the intermediate formation of HB, it was also inspected from different substrates: HA plus EtOH (**Figure 3A**) and H_2 plus HA (**Figure 3B**). The first reaction studied (**Table 1, R4**) was thermodynamically feasible under all considered conditions, being the best combination 25 °C, pH 7 and 1:3 HA:EtOH mass ratio. In this case, the pH and HB accumulation were revealed to be the most important parameters for its spontaneity, crossing the limit under pH <5 and [HB] >1M. The second reaction (**Table 1, R6**) was not spontaneous provably due to the low solubility of H_2 that limits its bioavailability in the liquid phase, though as stated by Liu et al. (2016), low pH slightly diminished $\Delta G'$ values. Besides, the developed model predicted that under low temperature (25 °C), high H_2:HA ratios (1:50), low amounts of HB ($<10^{-6}$ M) and high amounts of substrates ($[H_2] > 0.02$ M and [HA] > 0.1 M), the hydrogenotrophic HB formation could also become spontaneous.

Coinciding with the literature (Spirito et al., 2014; Wang et al., 2020), HC production was propitious under both studied situations (**Figure 4**). The same working conditions (25 °C, pH 7 and high EtOH concentration) thermodynamically prosper both reactions (**Table 1, R5 and R7**),

favouring its formation over intermediates as HB. However, the product accumulation had more impact compared to the previous reaction for HB production, and a lower amount (0.45 M) of HC was enough to switch its spontaneity. HC from HB and EtOH (**Figure 4A**) was less favourable than with HA and EtOH (**Figure 4B**). Those results oppose what is claimed in previous studies (Cavalcante et al., 2017) but it can be attributed to the ATP needed for EtOH oxidation in the overall coupled reaction (Wang et al., 2020). Nonetheless, when HB and EtOH worked as substrates (**Table 1, R5**), the effect of temperature was lower (0.4 *ΔG'* units per °C) compared to when HA and EtOH were used (**Table 1, R7**), in which *ΔG'* values increased 0.8 units per degree. Furthermore, reactions R4, R5 and R7 (**Table 1**) should be considered as H_2 is on the product side, so unlike the rest of the reactions, high P_{H_2} negatively affects their spontaneity.

Nevertheless, ButOH and HexOH (see supplementary material), whose emergence would decrease the selectivity of the process, were not thermodynamically feasible. High reducing power was needed for both to favour their production (Agler et al., 2011), though the concentration of their corresponding acids (HB and HC, respectively) turned out to be more pivotal than the accumulation of H_2. Besides low temperature (25 °C), low pH (5) boosted the two reactions (**Table 1, R8 and R9**) since an acidic pH favors the direction of the reactions to move towards the product side to reach equilibrium. Even though *ΔG'* values were positive, under the same studied conditions HexOH formation was slightly more reinforced compared to ButOH. However, their thermodynamic behavior among variables followed the same trend. Obtained results are consistent with previously reported data (Agler et al., 2011).

Altogether, after considering the working conditions, the modified Gibbs free energies were less favourable compared to the standard ones. The ionic strength of the solution had the lowest influence on the spontaneity of the reactions. On the other hand, the low solubility of the gases was the most decisive factor when these were used as substrates, for which HA was the only thermodynamically favourable compound from H_2 and CO_2 (**Table 2**). All studied reactions were

enhanced at low temperatures (like standard conditions), possibly due to their negative enthalpy increase in the range studied, since an increase in temperature caused an increase in *ΔG'*, reducing the spontaneity. Theoretically, 25 °C, pH 7 and high EtOH availability were aligned for the successive CO_2 elongation to HC. However, EtOH formation constituted a limitation for this purpose and the recalculated *ΔG'* values at different operational conditions are only theoretical, which means that there is no guarantee for microbial reactions to occur. In real systems, especially those in which biocatalysts are employed, many other factors as energy losses due to product inhibition and counter ion transport, genome, proteome and reaction kinetics that influence the microbial activity are involved (Korth and Harnisch, 2019). Yet, if the circumstances are given and the reactions take place, it should occur under the best thermodynamic conditions. Therefore, the set of parameters disentangled as optimal for HC formation was experimentally tested and evaluated.

3.2 Experimental tests to validate the thermodynamic outputs

HA and EtOH were needed as the main substrates to achieve the biological production of HC from CO_2. Different pHs (5, 6, 7) and temperatures (25, 37, 50 °C) were tested with the purpose to validate the results of the thermodynamic model (see supplementary material). HA was produced under any of the applied conditions, while EtOH was not. In natural systems, *ΔG'* of at least – 20 kJ mol^{-1} is required to consider a reaction as spontaneous (Smeaton and Van Cappellen, 2018). High temperatures may increase the rate of reactions but at the same time, they may exclude some microbial cultures from the game (Rovira-Alsina et al., 2020). Thus, a compromise between thermodynamics, kinetics, and biology (pH 7, 50 °C and high P_{H_2}) turned out to be the best combination for a fast HA generation (see supplementary material). On the contrary, EtOH formation has been reported as a constraint for these systems (Bian et al., 2020). Even though its production was also tested under 37 °C to favour microbial activity (Ghysels et al., 2021), no EtOH was obtained either from H_2 and CO_2 or from H_2 and HA (see supplementary material). However, other studies stated the ability to produce EtOH using

different technologies and substrates (Blasco-Gómez et al., 2019), eventually using the route proposed by de Leeuw and co-workers (2021). Since in the present scenario only HA was obtained (see supplementary material), EtOH was externally supplied in the following experiments.

Two fermenters were operated in duplicate for HC formation under the best thermodynamic conditions (pH 7, 25 °C, HA:EtOH of 1 to 3 g L^{-1}) and sparged with a gas mixture of CO_2:H_2 (20:80 *v/v*) under 1 bar of overpressure (**Figure 5, F1**) to keep an anaerobic atmosphere and the continuous HA generation. During the first 15 days of operation, no production was registered but the optical density linearly increased, which could be attributed to microbial growth. After that period, elongated compounds were obtained concomitantly with a higher increase in OD. HC was the main product, with a maximum concentration of 146.16 ± 1.73 mM C and a corresponding production rate of 12.45 ± 11.26 mM C d^{-1} (80.40 ± 53.42 mmol C g DCW^{-1} d^{-1}). Besides, HB was also observed, reaching a maximum concentration of 19.38 ± 11.98 mM C and a peak production rate of 2.28 ± 0.41 mM C d^{-1} (27.81 ± 15.11 mmol C g DCW^{-1} d^{-1}). Other compounds such as ButOH and HexOH were also present at the end of the test, but the sum of their concentrations was below 5 mM C. Based on the stoichiometry of the proposed reactions to accomplish HC production (**Table 1**, **R4 and R5 or R7**) and considering that EtOH is the only compound that was consumed but not produced, 2.4 moles were the minimum amount required to obtain 1 mole of HC. Considering an initial and final concentration of 86 and 15 mM of EtOH respectively, the maximum theoretical HC that could be produced in this test was 29 mM (176 mM C), meaning that only 30 mM C remained unconverted in the form of other compounds.

However, a set of conditions was sought to optimize HC production rates that were not only thermodynamically favourable but also closer to the biological complexity of these systems. Therefore, a second test at 37 °C was carried out in duplicate (**Figure 5, F2**). Selected conditions

corresponded to the optimum temperature for microbial activity and the second-best model output. During the first 7 days of operation, most of the EtOH was consumed to produce HB and HC, while it was fully consumed after 14 days, so 130 mMC extra of EtOH were supplied. It must be noted that by increasing the temperature the carbon build-up was enhanced. It is likely that as the thermodynamic model disclosed, the shortage of EtOH together with the high availability of HB and HC may have caused a shift in the metabolic pathways for the formation of these acids to the solventogenesis of their corresponding alcohols, decreasing the selectivity of the final spectrum. Even though they were not thermodynamically feasible, small amounts of ButOH and HexOH appeared to be produced thereafter. It has also been reported in previous studies, indicating that few microorganisms have the ability to trigger these reactions, possibly employing energy obtained in other simultaneous reactions (Pinto et al., 2021). The maximum concentrations of organic substances reached were as follows: 50.11 ± 4.77 mM C of HB, 253.25 ± 13.82 mM C of HC, 7.74 ± 10.95 of ButOH and 46.35 ± 55.00 mM C of HexOH. Other compounds accounted for less than 10 mM C. Nonetheless, HC was the main compound obtained at a maximum production rate of 25.08 ± 7.08 mM C d^{-1} (137.05 ± 1.71 mmol C g DCW^{-1} d^{-1}) and with a selectivity of 67 %. The results matched with expectations as operating under higher temperatures, higher production rates were anticipated (Rovira-Alsina et al., 2020). Here, considering an available concentration of 260 mMC of EtOH (initial plus added) and a non-converted concentration of 55 mM C, 256 mM C of HC could theoretically have been produced. However, the maximum was reached halfway through the test (day 15) and part of the HC was oxidized back to shorter compounds or converted to HexOH.

Following the results of the thermodynamic model, high P_{H_2} was expected to favour the formation of HA (**Table 2**) while low partial pressures were of interest to obtain HB and HC. Successive chain elongation steps consume and decrease the H_2 concentration. Therefore, it was periodically added in the system sparged together with CO_2 in previous tests to maintain available reducing power and a balanced microbial community composition (Paquete et al.,

2022). Here, an additional test (**Figure 6**) was performed under the same conditions as F2 with the only difference of the periodic modification of the P_{H_2} (from 0.60 to 1.80 atm) to optimize all the stages required for the elongation of HA and EtOH to HC. However, a certain amount was always kept in the system since its presence is a major selective factor in the microbial community.

Variable P_{H_2} could have accelerated the process since a similar concentration of HC as at the end of test F2 was obtained in less than 10 days. The maximum concentration and production rate of HC were 583.52 ± 17.82 mM C (11.30 ± 0.35 g L^{-1}) and 95.53 ± 3.19 mM C d^{-1} (1.85 ± 0.12 g L^{-1} d^{-1}, 565.96 ± 163.12 mmol C g DCW^{-1} d^{-1}) respectively, substantially higher than those of F2, while there was less residual HB. These results are in the range with the theoretical (maximum of 593 mMC of HC) and competitive with those achieved when performing in-line extraction (Kucek et al., 2016), as HB can act as an intermediate in favour of the formation of HC. In addition, some HA was accumulated over time, putatively both by its hydrogenotrophic formation and by the oxidation of EtOH, also necessary to address chain elongation (De Leeuw et al., 2019) but in lower amounts. This test evidenced that the highest HC yields were related to low P_{H_2} (days 8, 38 and 44), while the cases where this was not applicable can be attributed to a punctual decrease in pH due to the high microbial activity and the consequent accumulation of acids, that may have caused the solventogenesis of HB and HC into their respective alcohols (ButOH and HexOH, i.e. days 13 and 21). Nevertheless, HC was the main compound accounting for over 77 % of the total carbon at the end of the experiment, which represented an increase in selectivity of 10 % compared to the previous test (F2). The optical density followed a similar trend to F2, with a remarkable growth early on of the experiment, which was then presumably limited due to the lack of EtOH (day 8). Despite this, it was able to rebound to the maximum values acquired so far (> 0.4 AU) together with the maximum HC production for this study.

3.3 Implications of the developed approach

The theoretical best operational conditions using the thermodynamic-based model were assessed experimentally (see supplementary material). HA formation was thermodynamically feasible under any given conditions and it was experimentally validated, although temperature ruled out the best theoretical scenario due to its impact on reaction rates. Keeping a high P_{H_2} was crucial since a thermodynamic bottleneck may exist at low P_{H_2}, where hydrogenotrophic acetogenesis can be reversible (Ni et al., 2011). On the other hand, EtOH production was not feasible probably due to not all acetogens are capable to couple EtOH formation with net ATP gain (Candry et al., 2020). Finally, the parameters for the formation of HC matched except for the optimal temperature. 37 °C resulted to be better than 25 °C, as higher temperatures enhance the kinetics of the reactions, but as indicated by Spirito et al. (2014), 50 °C was fatal for biological chain elongation, hypothesizing enzyme inactivation. Therefore, temperature adequacy is of vital importance to enhance the desired reactions and ultimately produce elongated organic compounds.

Some authors suggested that concentrations of HC higher than 7.5 mM can have inhibitory effects on microbiological communities (Wu et al., 2020). Despite this, the concentration reached in the present study clearly exceeded this threshold, reaching concentrations more than 10 times higher (97mM) without compromising its production. This discrepancy could be attributable to pH, which modifies the equilibrium between the dissociated and undissociated forms and to strain-specific inhibition thresholds, as postulated by Ramió-Pujol and co-workers (2015). Furthermore, a kinetic and thermodynamic modeling analysis (González-Cabaleiro et al., 2013) suggested that direct conversion of HA to MCCA by H_2 was very unlikely to be attainable even under high P_{H_2}. Here, direct HC from H_2 and CO_2 could not be experimentally achieved (see supplementary material). Though, the indirect generation via sequential pathways in a single

reactor may also be slowed down by the different conditions required for HA formation, the kinetics of which depends mainly on the soluble gas.

Overall, chain elongation reactions represented favorable thermodynamics for all carboxylates despite alcohols, usually with a lower energy gain when H_2 was present. Experimentally, the best configuration to obtain HC could be the formation of its main substrates and its subsequent elongation in two separate steps (Romans-Casas et al., 2021). The integration of the knowledge obtained through the model and its inference to perform experimental tests helped to define and apply the most favorable conditions for each reaction, thus obtaining the highest concentration of HC so far from simple compounds. Besides, this approach provides insights on the importance of merging key factors to study biological processes and consider them as a complex network of constantly changing interactions.

4. Conclusions

The present work addresses some concerns for the screening of operating parameters in chain elongation processes. Thermophilic conditions reinforced HA formation, EtOH production was the limiting step and longer carbon compounds were only obtained at mid temperatures. Particularly, HC was boosted under 37 °C, pH 7 and 1:3 (HA:EtOH) ratio, especially with intermittently P_{H_2} decrease. This study enlightens the differences between thermodynamic projections and experimental results, which enabled to optimize the working parameters and to obtain the highest HC concentration from single substrates. However, given the intrinsic characteristics of each compound, further investigation is required to maximize the target-product selectivity.

Tables and figures

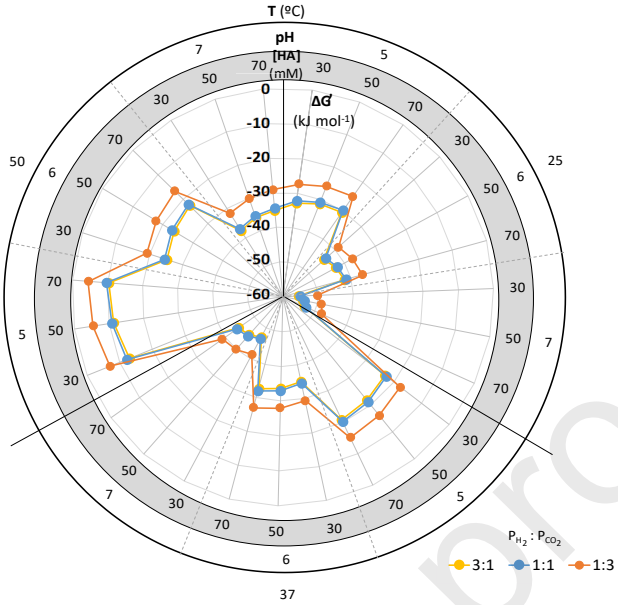

R1: $4H_2 + 2CO_2 \rightarrow CH_3COO^- + H^+ + 2H_2O$

Figure 1. Gibbs free energy variation (*ΔG'*) for hydrogenotrophic acetic acid (HA) formation. Different conditions of pH, temperature (T; °C), substrates ratios (P_{H_2} and P_{CO_2}; H_2 and CO_2 partial pressures respectively, in atm) and product concentration ([HA] in mM) were tested.

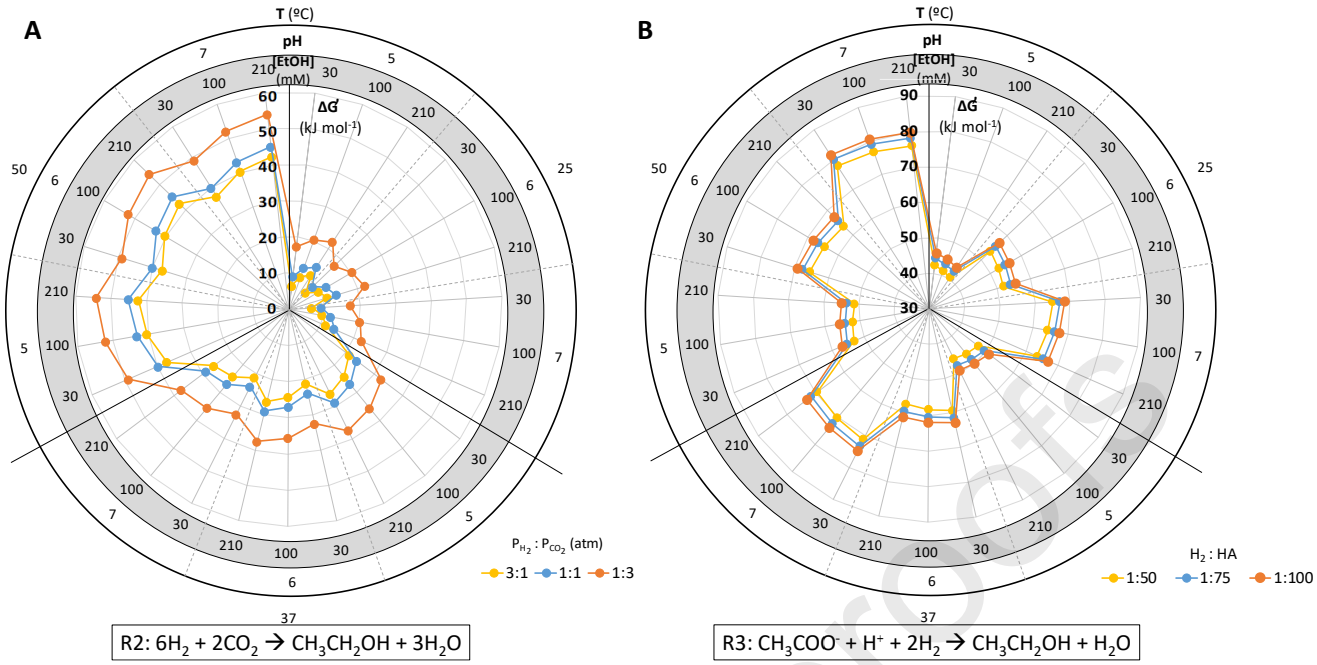

Figure 2. Gibbs free energy variation ($\Delta G'$) for hydrogenotrophic ethanol (EtOH) formation (A) and acetic acid (HA) conversion to ethanol (B). Different conditions of pH, temperature (T; °C), substrates ratios (P_{H_2} and P_{CO_2}; H_2 and CO_2 partial pressures respectively, in atm, or HA and H_2 in M) and product concentration ([EtOH] in mM) were tested.

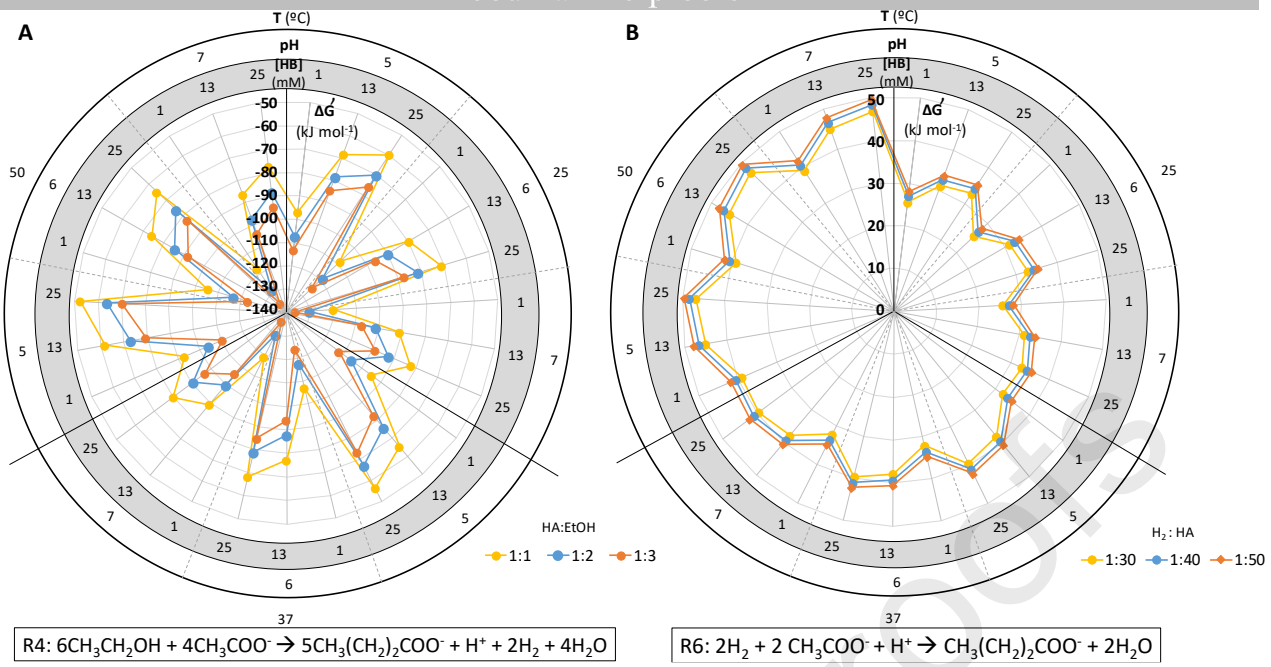

R4: $6CH_3CH_2OH + 4CH_3COO^- \rightarrow 5CH_3(CH_2)_2COO^- + H^+ + 2H_2 + 4H_2O$

R6: $2H_2 + 2\ CH_3COO^- + H^+ \rightarrow CH_3(CH_2)_2COO^- + 2H_2O$

Figure 3. Gibbs free energy variation (*ΔG'*) for n-butyric acid (HB) production from HA and EtOH (A) or HA and H_2 (B). Different conditions of pH, temperature (T; °C), substrate ratios in molar (M) units, and product concentration ([HB] in mM) were tested.

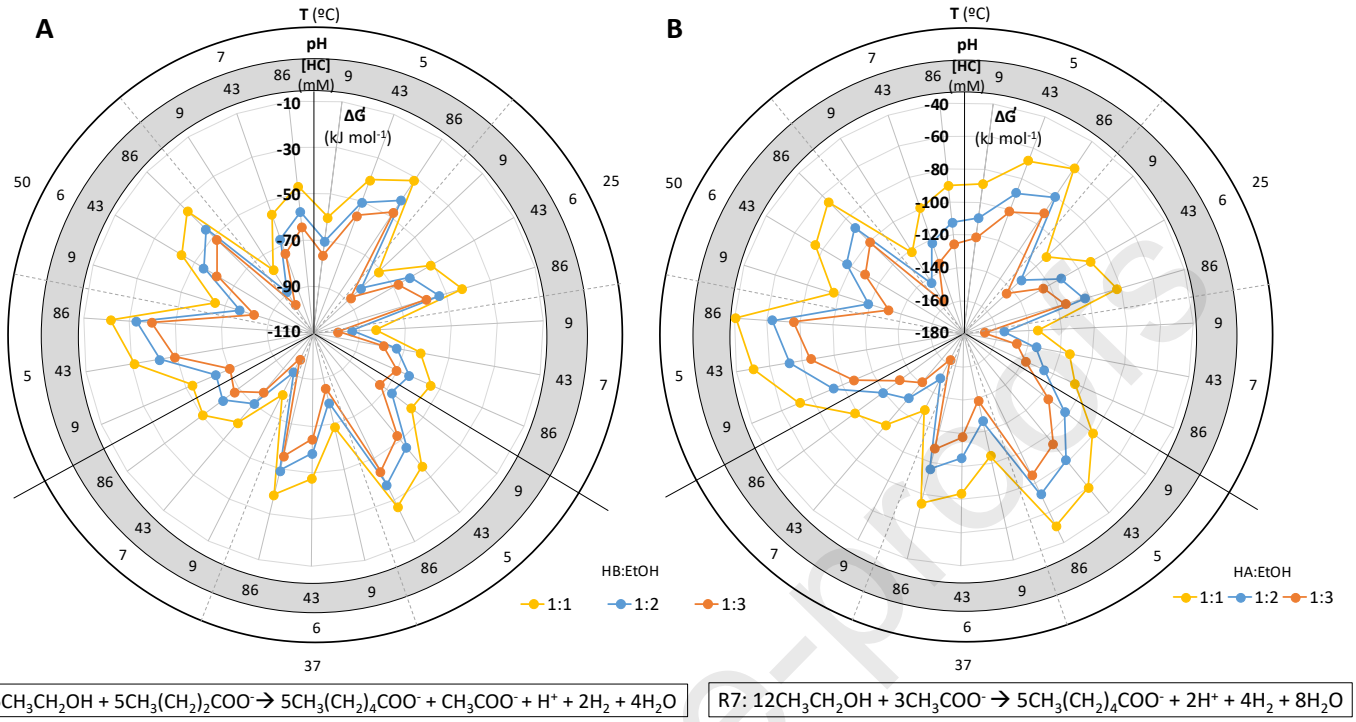

R5: $6CH_3CH_2OH + 5CH_3(CH_2)_2COO^- \rightarrow 5CH_3(CH_2)_4COO^- + CH_3COO^- + H^+ + 2H_2 + 4H_2O$

R7: $12CH_3CH_2OH + 3CH_3COO^- \rightarrow 5CH_3(CH_2)_4COO^- + 2H^+ + 4H_2 + 8H_2O$

Figure 4. Evolution of Gibbs free energy (*ΔG'*) for n-caproic acid (HC) formation from EtOH and HB (A) or HA (B). Different conditions of pH, temperature (T; °C), substrate ratios (M) and product concentration ([HC] in mM) were tested.

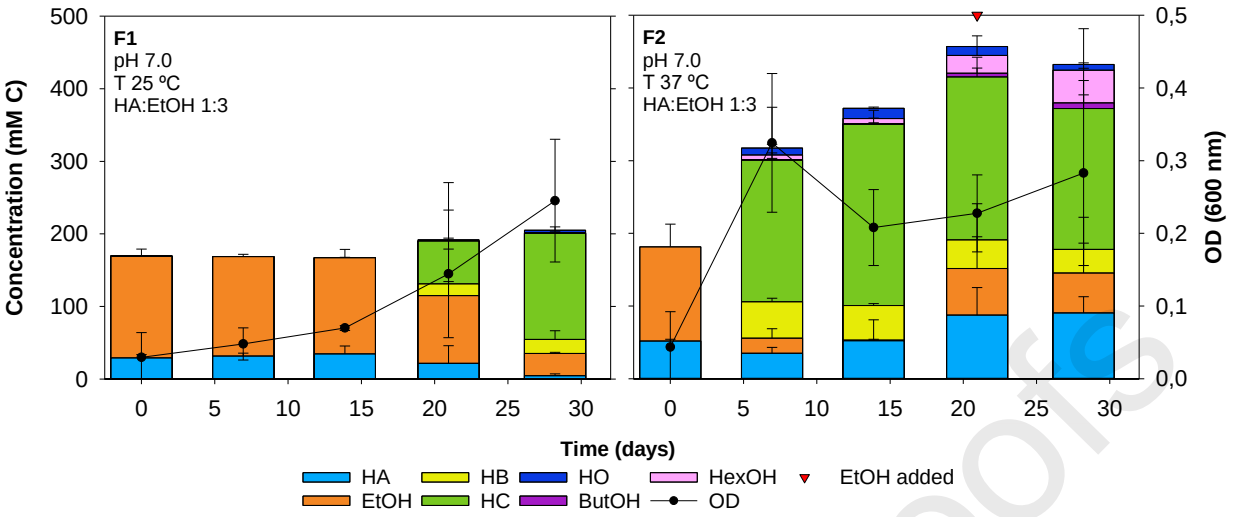

Figure 5. Evolution of carbon compounds in the first (F1) and second (F2) fermentative tests. F1 was operated under the most suitable conditions unraveled by the thermodynamic model to trigger caproic acid production. F2 was performed with the aim to optimize chain elongation considering biological factors. HA: acetic acid, EtOH: ethanol, HB: n-butyric acid, HC: n-caproic acid, ButOH: n-butanol, HexOH: n-hexanol and OD: optical density. The red inverted triangle points out extra ethanol addition.

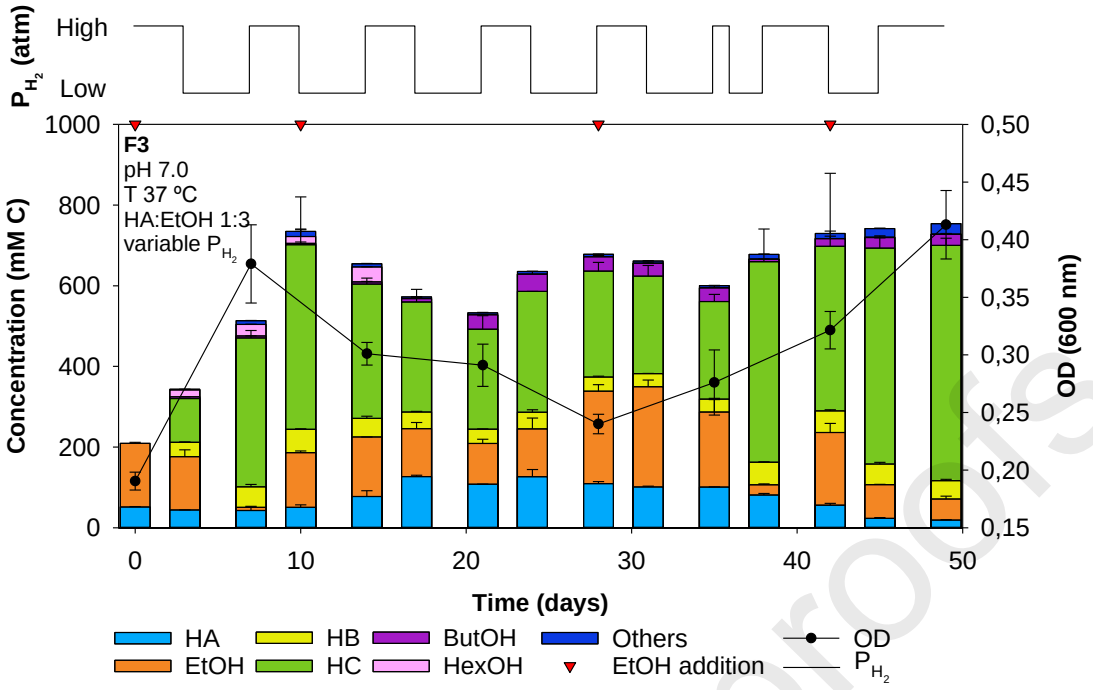

Figure 6. Evolution of carbon compounds in the third fermentative test (F3) working under the same operational conditions as F2 but periodically varying the H_2 partial pressure. HA: acetic acid, EtOH: ethanol, HB: n-butyric acid, HC: n-caproic acid, ButOH: n-butanol, HexOH: n-hexanol, OD: optical density, P_{H_2}: hydrogen partial pressure. Inverted triangles indicate external ethanol addition.

Table 1. Standard Gibbs free energy (ΔG°) change for gas fermentation and chain elongation reactions. For chain elongation reaction with ethanol oxidation, the overall coupled reaction is shown and used for the calculations below.

	Reaction		ΔG°_{25} (kJ mol^{-1})	Source
Gas fermentation	R1	Hydrogenotrophic acetogenesis $4H_2 + 2CO_2 \rightarrow CH_3COO^- + H^+ + 2H_2O$	-94.96	(Spirito et al., 2014)
	R2	Hydrogenotrophic solventogenesis $6H_2 + 2CO_2 \rightarrow CH_3CH_2OH + 3H_2O$	-105.00	(Baleeiro et al., 2019)
Chain elongation	R3	Acetate reduction to ethanol with H_2 $CH_3COO^- + H^+ + 2H_2 \rightarrow CH_3CH_2OH + H_2O$	-10.50	(Spirito et al., 2014)
	R4	Ethanol-acetate elongation to n-butyrate $6CH_3CH_2OH + 4CH_3COO^- \rightarrow 5CH_3(CH_2)_2COO^- + H^+ + 2H_2 + 4H_2O$	-28.75	(Wang et al., 2020)
	R5	Ethanol-butyrate elongation to n-caproate $6CH_3CH_2OH + 5CH_3(CH_2)_2COO^- \rightarrow 5CH_3(CH_2)_4COO^- + CH_3COO^- + H^+ + 2H_2 + 4H_2O$	-36.7	(Spirito et al., 2014)
	R6	Hydrogenotrophic acetate elongation to n-butyrate $2H_2 + 2\ CH_3COO^- + H^+ \rightarrow CH_3(CH_2)_2COO^- + 2H_2O$	-48.20	(Baleeiro et al., 2019)
	R7	Ethanol-acetate elongation to n-caproate $12CH_3CH_2OH + 3CH_3COO^- \rightarrow 5CH_3(CH_2)_4COO^- + 2H^+ + 4H_2 + 8H_2O$	-57.60	(Wang et al., 2020)
	R8	n-butyrate elongation to n-butanol $CH_3(CH_2)_2COO^- + H^+ + 2H_2 \rightarrow CH_3(CH_2)_3OH + H_2O$	-6.46	(Agler et al., 2011)*
	R9	n-caproate elongation to n-hexanol $CH_3(CH_2)_4COO^- + H^+ + 2H_2 \rightarrow CH_3(CH_2)_5OH + H_2O$	-10.33	(Agler et al., 2011)*

ΔG° activities equal to 1 and pH 7

* Recalculated from ΔG values at 37°C

Table 2. Compilation of the thermodynamic analysis outputs for the formation of each compound.

Spontaneous reactions are colored in green, while non-spontaneous ones are colored in red.

Compound			Energy requirements	Optimal thermodynamic conditions		
				pH	T (°C)	Substrate
Acetic acid	$H_2 + CO_2$	(R 1)	Spontaneous	7	25	High P_{H_2}
Ethanol	$H_2 + CO_2$	(R 2)	Requires Energy	5	25	High P_{H_2}
	H_2 + HA	(R 3)				High HA
n-Butyric acid	HA + EtOH	(R 4)	Spontaneous	7	25	High EtOH
	HA + H_2	(R 6)	Requires energy	5		High P_{H_2}
n-Caproic acid	HB + EtOH	(R 5)	Spontaneous	7	25	High EtOH
	HA + EtOH	(R 7)				
n-Butanol	(R 8)		Requires energy	5	25	High HB
n-Hexanol	(R 9)		Requires energy	5	25	High HC

E-supplementary data for this work can be found in e-version of this paper online.

Declaration of interests

☒ The authors declare that they have no known competing financial interests or personal relationships that could have appeared to influence the work reported in this paper.

Acknowledgments

The authors acknowledge funding from the Agency for Business Competitiveness of the Government of Catalonia (ACCIÓ; COMRDI16-1-0061) and the Spanish Ministry of Science and Innovation (RTI2018-098360-B-100 and PLEC2021-007802). LEQUIA (http://www.lequia.udg.edu/) has been recognized as a consolidated research group by the Catalan Government (2017-SGR-1552). L.R.-A. acknowledge the support by the Catalan Government (2018 FI-B 00347) in the European FSE program (CCI 2014ES05SFOP007). M.R.-C. is grateful for the support of the Spanish Government (FPU20/01362). S.P is a Serra Hunter Fellow (UdG-AG-575) and acknowledges the funding from the ICREA Academia award.

5. References

1. Agler, M.T., Wrenn, B.A., Zinder, S.H., Angenent, L.T., 2011. Waste to bioproduct conversion with undefined mixed cultures: The carboxylate platform. Trends Biotechnol. 29 (2), 70–78. 10.1016/j.tibtech.2010.11.006

2. Alberty, R.A., 2001. Effect of temperature on standard transformed Gibbs energies of formation of reactants at specified pH and ionic strength and apparent equilibrium constants of biochemical reactions. J. Phys. Chem. B 105 (32), 7865–7870. 10.1021/jp011308v

3. Amend, J.P., Shock, E.L., 2001. Energetics of overall metabolic reactions of thermophilic and hyperthermophilic Archaea and Bacteria. FEMS Microbiol. Rev. 25 (2), 175–243.

10.1016/S0168-6445(00)00062-0

4. Angenent, L.T., Richter, H., Buckel, W., Spirito, C.M., Steinbusch, K.J.J., Plugge, C.M., Strik, D.P.B.T.B., Grootscholten, T.I.M., Buisman, C.J.N., Hamelers, H.V.M., 2016. Chain Elongation with Reactor Microbiomes : Open-Culture Biotechnology To Produce Biochemicals 50 (6), 2796-2810. 10.1021/acs.est.5b04847

5. Baleeiro, F.C.F., Kleinsteuber, S., Neumann, A., Sträuber, H., 2019. Syngas-aided anaerobic fermentation for medium-chain carboxylate and alcohol production: the case for microbial communities. Appl. Microbiol. Biotechnol. 103 (21-22), 8689–8709. 10.1007/s00253-019-10086-9

6. Bian, B., Bajracharya, S., Xu, J., Pant, D., Saikaly, P.E., 2020. Microbial Electrosynthesis from CO2: Challenges, opportunities and perspectives in the context of circular bioeconomy. Bioresour. Technol. 302, 122863. 10.1016/j.biortech.2020.122863

7. Blasco-Gómez, R., Ramió-Pujol, S., Bañeras, L., Colprim, J., Balaguer, M.D., Puig, S., 2019. Unravelling the factors that influence the bio-electrorecycling of carbon dioxide towards biofuels. Green Chem. 21, 684–691. 10.1039/c8gc03417f

8. Blasco-Gómez, R., Romans-casas, M., Bolognesi, S., Perona-vico, E., Colprim, J., Balaguer, M.D., Puig, S., 2021. Steering bio-electro recycling of carbon dioxide towards target compounds through novel inoculation and feeding strategies. J. Environ. Chem. Eng. 9 (4), 105549. 10.1016/j.jece.2021.105549

9. Candry, P., Ganigué, R., 2021. Chain elongators, friends, and foes. Curr. Opin. Biotechnol. 67, 99–110. 10.1016/j.copbio.2021.01.005

10. Candry, P., Huang, S., Carvajal-Arroyo, J.M., Rabaey, K., Ganigue, R., 2020. Enrichment and characterisation of ethanol chain elongating communities from natural and engineered environments. Sci. Rep. 10 (3682), 1–10. 10.1038/s41598-020-60052-z

11. Cavalcante, W. de A., Leitão, R.C., Gehring, T.A., Angenent, L.T., Santaella, S.T., 2017. Anaerobic fermentation for n-caproic acid production: A review. Process Biochem. 54, 106–119. 10.1016/j.procbio.2016.12.024

12. de Leeuw, K.D., Ahrens, T., Buisman, C.J.N., Strik, D.P.B.T.B., 2021. Open Culture Ethanol-Based Chain Elongation to Form Medium Chain Branched Carboxylates and Alcohols. Front. Bioeng. Biotechnol. 9 (697439), 2296–4185. 10.3389/fbioe.2021.697439

13. de Leeuw, K.D., Buisman, C.J.N., Strik, D.P.B.T.B., 2019. Branched Medium Chain Fatty Acids: Iso-Caproate Formation from Iso-Butyrate Broadens the Product Spectrum for Microbial Chain Elongation. Environ. Sci. Technol. 53 (13), 7704–7713. 10.1021/acs.est.8b07256

14. Dessì, P., Rovira-Alsina, L., Sánchez, C., Dinesh, G.K., Tong, W., Chatterjee, P., Tedesco, M., Farràs, P., Hamelers, H.M.V., Puig, S., 2021. Microbial electrosynthesis: Towards sustainable biorefineries for production of green chemicals from CO_2 emissions. Biotechnol. Adv. 46, 107675. 10.1016/j.biotechadv.2020.107675

15. Dürre, P., Eikmanns, B.J., 2015. C1-carbon sources for chemical fuel production by microbial gas fermentation. Curr. Opin. Biotechnol. 35, 63–72. 10.1016/j.copbio.2015.03.008

16. Ghysels, S., Buffel, S., Rabaey, K., Ronsse, F., Ganigué, R., 2021. Biochar and activated carbon enhance ethanol conversion and selectivity to caproic acid by Clostridium kluyveri. Bioresour. Technol. 319, 124236. 10.1016/j.biortech.2020.124236

17. Gildemyn, S., Rozendal, R.A., Rabaey, K., 2017. A Gibbs Free Energy-Based Assessment of Microbial Electrocatalysis. Trends Biotechnol. 35 (5), 393–406. 10.1016/j.tibtech.2017.02.005

18. Goldberg, R.N., Tewari, Y.B., 1991. Thermodynamics of the disproportionation of adenosine 5′-diphosphate to adenosine 5′-triphosphate and adenosine 5′-monophosphate. I. Equilibrium model. Biophys. Chem. 40 (3), 241–261. 10.1016/0301-4622(91)80024-L

19. González-Cabaleiro, R., Lema, J.M., Rodríguez, J., Kleerebezem, R., 2013. Linking

thermodynamics and kinetics to assess pathway reversibility in anaerobic bioprocesses. Energy Environ. Sci. 6 (12), 3780–3789. 10.1039/c3ee42754d

20. Grootscholten, T.I.M., Steinbusch, K.J.J., Hamelers, H.V.M., Buisman, C.J.N., 2013. Chain elongation of acetate and ethanol in an upflow anaerobic filter for high rate MCFA production. Bioresour. Technol. 135, 440–445. 10.1016/j.biortech.2012.10.165

21. Hanselmann, K.W., 1991. Microbial energetics applied to waste repositories. Experientia 47, 645–687. 10.1007/BF01958816

22. Kleerebezem, R., Van Loosdrecht, M.C.M., 2010. A generalized method for thermodynamic state analysis of environmental systems. Crit. Rev. Environ. Sci. Technol. 40 (1), 1–54. 10.1080/10643380802000974

23. Korth, B., Harnisch, F., 2019. Modeling microbial electrosynthesis. Adv. Biochem. Eng. Biotechnol. 167, 273–325. 10.1007/10_2017_35

24. Kucek, L.A., Nguyen, M., Angenent, L.T., 2016. Conversion of L-lactate into n-caproate by a continuously fed reactor microbiome. Water Res. 93, 163–171. 10.1016/j.watres.2016.02.018

25. Lambrecht, J., Cichocki, N., Schattenberg, F., Kleinsteuber, S., Harms, H., Müller, S., Sträuber, H., 2019. Key sub-community dynamics of medium-chain carboxylate production. Microb. Cell Fact. 18 (92), 1–18. 10.1186/s12934-019-1143-8

26. Lide, D.R., Baysinger, G., 2004. CRC handbook of chemistry and physics: a ready-reference book of chemical and physical data. Choice Rev. Online 41 (8), 41-4368-41–4368. 10.5860/choice.41-4368

27. Liu, Y., Lü, F., Shao, L., He, P., 2016. Alcohol-to-acid ratio and substrate concentration affect product structure in chain elongation reactions initiated by unacclimatized inoculum. Bioresour. Technol. 218, 1140–1150. 10.1016/j.biortech.2016.07.067

28. Ni, B.J., Liu, H., Nie, Y.Q., Zeng, R.J., Du, G.C., Chen, J., Yu, H.Q., 2011. Coupling glucose fermentation and homoacetogenesis for elevated acetate production: Experimental and mathematical approaches. Biotechnol. Bioeng. 108 (2), 345–353. 10.1002/bit.22908

29. Paquete, C.M., Rosenbaum, M.A., Bañeras, L., Rotaru, A.E., Puig, S., 2022. Let's chat: Communication between electroactive microorganisms. Bioresour. Technol. 347, 126705. 10.1016/j.biortech.2022.126705

30. Pinto, T., Flores-Alsina, X., Gernaey, K.V., Junicke, H., 2021. Alone or together? A review on pure and mixed microbial cultures for butanol production. Renew. Sustain. Energy Rev. 147, 111244. 10.1016/j.rser.2021.111244

31. Ramió-Pujol, S., Ganigué, R., Bañeras, L., Colprim, J., 2015. Incubation at 25°C prevents acid crash and enhances alcohol production in Clostridium carboxidivorans P7. Bioresour. Technol. 192, 296–303. 10.1016/j.biortech.2015.05.077

32. Romans-Casas, M., Blasco-Gómez, R., Colprim, J., Balaguer, M.D., Puig, S., 2021. Bio-electro CO2 recycling platform based on two separated steps. J. Environ. Chem. Eng. 9 (5), 105909. 10.1016/j.jece.2021.105909

33. Rovira-Alsina, L., Perona-Vico, E., Bañeras, L., Colprim, J., Balaguer, M.D., Puig, S., 2020. Thermophilic bio-electro CO_2 recycling into organic compounds. Green Chem. 22 (9), 2947-2955. 10.1007/978-3-540-74382-8_4

34. Smeaton, C.M., Van Cappellen, P., 2018. Gibbs Energy Dynamic Yield Method (GEDYM): Predicting microbial growth yields under energy-limiting conditions. Geochim. Cosmochim. Acta 241, 1–16. 10.1016/j.gca.2018.08.023

35. Spirito, C.M., Richter, H., Rabaey, K., Stams, A.J.M., Angenent, L.T., 2014. Chain elongation in anaerobic reactor microbiomes to recover resources from waste. Curr. Opin. Biotechnol. 27, 115–122. 10.1016/j.copbio.2014.01.003

36. Vassilev, I., Dessì, P., Puig, S., Kokko, M., 2022. Cathodic biofilms – A prerequisite for microbial electrosynthesis. Bioresour. Technol. 348, 126788. 10.1016/j.biortech.2022.126788

37. Wang, Q., Zhang, P., Bao, S., Liang, J., Wu, Y., Chen, N., Wang, S., Cai, Y., 2020. Chain elongation performances with anaerobic fermentation liquid from sewage sludge with high total solid as electron acceptor. Bioresour. Technol. 306, 123188. 10.1016/j.biortech.2020.123188

38. Wood, J.C., Grové, J., Marcellin, E., Heffernan, J.K., Hu, S., Yuan, Z., Virdis, B., 2021. Strategies to improve viability of a circular carbon bioeconomy-A techno-economic review of microbial electrosynthesis and gas fermentation. Water Res. 201, 117306. 10.1016/j.watres.2021.117306

39. Wu, Q., Guo, W., Bao, X., Meng, X., Yin, R., Du, J., Zheng, H., Feng, X., Luo, H., Ren, N., 2018. Upgrading liquor-making wastewater into medium chain fatty acid: Insights into co-electron donors, key microflora, and energy harvest. Water Res. 145, 650-659. 10.1016/j.watres.2018.08.046

40. Wu, Q., Ren, W., Guo, W., Ren, N., 2022. Effect of substrate structure on medium chain fatty acids production and reactor microbiome. Environ. Res. 204 (A), 111947. 10.1016/j.envres.2021.111947

41. Wu, S.-L., Sun, J., Xueming, C., Wei, W., Song, L., Dai, X., Ni, B.-J., 2020. Unveiling the mechanisms of medium-chain fatty acid production from waste activated sludge alkaline fermentation liquor through physiological, thermodynamic and metagenomic investigations. Water Res. 169, 115218. 10.1016/j.watres.2019.115218

Declaration of interests

☒The authors declare that they have no known competing financial interests or personal relationships that could have appeared to influence the work reported in this paper.

☐The authors declare the following financial interests/personal relationships which may be

considered as potential competing interests:

42.

Declaration of interests

☒The authors declare that they have no known competing financial interests or personal relationships that could have appeared to influence the work reported in this paper.

☐The authors declare the following financial interests/personal relationships which may be considered as potential competing interests:

43.

Highlights

- The potential procurement of elongated compounds from CO_2 was studied and tested.
- The thermodynamic analysis revealed ethanol was the bottleneck for chain elongation
- Experimental tests allowed fine-tuning of the operating conditions
- The integration of thermodynamics and biology intensified caproic acid production
- The highest caproic acid titter (> 11 g L^{-1}) was obtained from simple substrates

44.

45.